nature catalysis

SUPPLEMENTARY INFORMATION

https://doi.org/10.1038/s41929-019-0289-4

In the format provided by the authors and unedited.

The atomic-resolution crystal structure of activated [Fe]-hydrogenase

Gangfeng Huang[1,8], Tristan Wagner[1,7,8], Matthew D. Wodrich[2,3], Kenichi Ataka[4], Eckhard Bill[5], Ulrich Ermler[6], Xile Hu[2] and Seigo Shima[1*]

[1]Microbial Protein Structure Group, Max Planck Institute for Terrestrial Microbiology, Marburg, Germany. [2]Laboratory of Inorganic Synthesis and Catalysis, Institute of Chemical Science and Engineering, Ecole Polytechnique Fédérale de Lausanne (EPFL), Lausanne, Switzerland. [3]Laboratory for Computational Molecular Design, Institute of Chemical Science and Engineering, Ecole Polytechnique Fédérale de Lausanne (EPFL), Lausanne, Switzerland. [4]Department of Physics, Freie Universität Berlin, Berlin, Germany. [5]Department Molecular Theory and Spectroscopy, Max Planck Institute for Chemical Energy Conversion, Mülheim an der Ruhr, Germany. [6]Department of Molecular Membrane Biology, Max Planck Institute of Biophysics, Frankfurt am Main, Germany. [7]Present address: Microbial Metabolism group, Max Planck Institute for Marine Microbiology, Bremen, Germany. [8]These authors contributed equally: Gangfeng Huang, Tristan Wagner. *e-mail: shima@mpi-marburg.mpg.de

Supplementary Information

The atomic-resolution crystal structure of activated [Fe]-hydrogenase

Gangfeng Huang[1]*, Tristan Wagner[1]*, Matthew D. Wodrich[2,3], Kenichi Ataka[4], Eckhard Bill[5], Ulrich Ermler[6], Xile Hu[2] and Seigo Shima[1]†

[1]Microbial Protein Structure Group, Max Planck Institute for Terrestrial Microbiology, Marburg, Germany. [2]Laboratory of Inorganic Synthesis and Catalysis, Institute of Chemical Science and Engineering, Ecole Polytechnique Fédérale de Lausanne (EPFL), Lausanne, Switzerland. [3]Laboratory for Computational Molecular Design, Institute of Chemical Science and Engineering, Ecole Polytechnique Fédérale de Lausanne (EPFL), Lausanne, Switzerland. [4]Department of Physics, Freie Universität Berlin, Berlin, Germany. [5]Department Molecular Theory and Spectroscopy, Max Planck Institute for Chemical Energy Conversion, Mülheim an der Ruhr, Germany. [6]Department of Molecular Membrane Biology, Max Planck Institute of Biophysics, Frankfurt am Main, Germany. *These authors contributed equally to this work. †e-mail: shima@mpi-marburg.mpg.de

Present address of Tristan Wagner: Microbial Metabolism group, Max Planck Institute for Marine Microbiology, Celsiusstraße 1, 28359 Bremen, Germany

Table of Content

Supplementary Methods

Chemicals. Tetrahydromethanopterin (H_4MPT) and methenyl-H_4MPT$^+$ were purified from *Methanothermobacter marburgensis* cells as described previously[1]. Methylene-H_4MPT was synthesized from H_4MPT by the reaction with formaldehyde[1]. Other chemical compounds were purchased from Carl Roth and Sigma-Aldrich.

Gene synthesis of [Fe]-hydrogenase from *Methanococcus aeolicus*. The [Fe]-hydrogenase gene from *M. aeolicus* (NCBI Reference Sequence: WP_011973735.1) is described below; the codon usage was optimized and synthesized by GenScript.

5′-

CATATGAAAGTAGCAATACTAGGAGCTGGGTGTTATAGGTCACACGCTGCATGTGGG
ATTACCAACTTTAGCCGTGCGGCGGAAGTGGCGAACAAAGTGGGCATTCCGGAAAT
CACCATGACCCACAGCACCATTACCATGGGTGCGGAGCTGCTGCACCTGGTTGACGA
GATCGATGAAGTGGTTGTGAGCGACCCGTGCTTTGCGGAGGAACCGGGTCTGATCAT
TATCGACGAATTTGATTGCAAAGAGGTGATGGAAGCGCATCTGGCGGGCAAGGCGG
AGGATGTGATGCCGGCGATTCGTGATGCGGTTAAGGCGAAAGCGAAGGATAGCCCG
AAACCGCCGAAGGGCTGCATCCACTTTGTGAACCCGGAAAAAGTTGGTCTGAAGGT
GACCAGCGACGATCGTGAGGCGATCGAAGGCGCGGACATTGTTATCACCTGGCTGCC
GAAGGGTGGCAGCCAGCCGGCGATTATCGAGAAATTCGTGGATGCGATTAAGGAAG
GCGCGATCGTTACCCACGCGTGCACCATTCCGACCCCGAAATTCGCGAAGATCTTTA
AAGACCTGGGTCGTGAGGATCTGAACATTGTTAGCTTTCACCCGGGTTGCGTGCCGG
AGATGAAAGGCCAAGTTTACCTGAGCGAAGGTTATGCGAGCGAGGAAGCGGTTGAG
AAGCTGTACAAAATTGCGAAGATCAGCCGTGGCACCGCGTTCAAGATGCCGGCGAA
CCTGATCAGCCCGGTGTGCGACATGGGTAGCGCGGTTACCGCGCCGGTGTATGCGGC

GATTCTGAGCTATCGTGATGCGGTTACCAACATTCTGGGTGCGCCGGCGGACTTTGC
GCAGATGATGGCGGATGAAGCGATTACCCAAATGCTGGAGCTGATGCGTAACGAAG
GTATCCAGAACATGGAGAACAAACTGAACCCGGGTGCGCTGACCGGTACCGCGGAC
AGCATGTGCTTCGGTCCGCTGAGCGAACTGCTGCCGGCGAGCCTGAAGGTTCTGGAG
GAACATAAAAAGTAAGTCGAC-3′

The DNA was synthesized and inserted into the expression vector pET-24b (+) at the NdeI and SalI restriction-enzyme digestion-sites. Genes of the mutants (M252A, M252F and M252S) were synthesized using the template of the wild-type [Fe]-hydrogenase gene.

Heterologous production of the apoenzyme of [Fe]-hydrogenase and its purification. The apoenzymes of [Fe]-hydrogenase (wild type and the mutants) were overproduced in *Escherichia coli* BL21(DE3). The recombinant *E. coli* was cultivated in the tryptone-phosphate (TP) medium[2] with 50-μg/ml kanamycin at 37 °C. The gene expression was started by addition of 1-mM isopropyl β-D-thiogalactopyranoside (IPTG) when the optical density at 600 nm became 0.6−0.8. The induction continued for 4 hours and the cells were harvested by centrifugation using Avanti JXN-26 centrifuge with JLA-10.500 rotor (Beckman-Coulter) at 8000 rpm for 30 min at 4 °C and the cells (~10 g) were resuspended in 50-mM 3-(N-morpholino)propanesulfonic acid (MOPS)/KOH pH 7.0 containing 1-mM dithiothreitol (DTT). The cells were disrupted by sonication using SONOPULS GM200 (Bandelin) with KE76 tip and 50 cycles on ice. The cell debris and the unbroken cells were removed by centrifugation using an Avanti JXN-26 centrifuge with a JA-25.50 rotor (Beckman-Coulter) at 15000 rpm for 30 min at 4 °C. Ammonium sulphate was added into the supernatant to the final concentration of 2 M, and incubated on ice for 10 min. The precipitation was removed by centrifugation using an Avanti JXN-26 centrifuge with JA-25.50 rotor (Beckman-Coulter) at 15000 rpm for 30 min at 4 °C. The supernatant was applied to

a Phenyl Sepharose High Performance column (75 ml, GE Healthcare Life Sciences) and eluted with a linear gradient of ammonium sulphate elution from 2 M to 0 M in 50-mM MOPS/KOH buffer pH 7.0 containing 1-mM DTT. Fractions containing the apoenzyme of [Fe]-hydrogenase were pooled and concentrated by using an Amicon Ultra-4 Centrifugation filter (30 kDa cut-off) (Millipore). Then the concentrated apoenzyme sample was applied to a HiPrep 16/60 Sephacryl S-200 HR gel filtration column (120 ml, GE Healthcare Life Sciences) equilibrated with 25-mM Tris(hydroxymethyl)aminomethane (Tris)/HCl buffer pH 7.5 containing 150-mM NaCl, 5% glycerol and 2-mM DTT. We repeated once the gel filtration using the same column and conditions to increase the purity of protein. Finally, the purified apoenzyme was concentrated to ~50 mg/ml and stored at −75 °C for the reconstitution. Protein concentration determination was performed using Bradford method using the assay solution from Bio-Rad Laboratories and bovine serum albumin as the standard.

Reconstitution of the [Fe]-hydrogenase holoenzyme. Purification of [Fe]-hydrogenase, extraction of the FeGP cofactor and reconstitution of the [Fe]-hydrogenase were performed under strictly anaerobic condition in the anaerobic chamber (Coy) containing the gas phase of 95%N_2/5%H_2 under yellow light as described previously[3]. The FeGP cofactor was extracted from [Fe]-hydrogenase purified from *M. marburgensis* as previously described [3]. To prepare the reconstituted holoenzyme, 1.0 ml of 2-mM FeGP cofactor and 1.0 ml of 1.46-mM apoenzyme of [Fe]-hydrogenase from *M. aeolicus* were mixed with 8 ml of 50-mM Tris/HCl pH 8.5. Then the mixture was incubated in the anaerobic tent at 8 °C for 30 min. Unbound FeGP cofactor was removed by washing with 10-mM MOPS/KOH pH 7.0 using Amicon Ultra-4 Centrifugation filter (30 kDa cut-off) (Millipore). Finally, the reconstituted holoenzyme was concentrated to ~50 mg/ml, which contains 10-mM MOPS/KOH pH 7.0 and stored at −75 °C for further use. Activity

assay and UV-Vis spectroscopy were performed to control the quality of the reconstituted holoenzyme, which has the absorbance peak of the Fe-complex at 360 nm (ref 3). The specific activity of the reconstituted [Fe]-hydrogenase holoenzyme showed 3000 U/mg using methylene-H_4MPT as the substrate in the assay containing 120-mM potassium phosphate buffer pH 6.0 and 1-mM ethylenediaminetetraacetic acid (EDTA).

Enzyme activity assay of [Fe]-hydrogenase. The activity of [Fe]-hydrogenase was measured as previously described, using 1-ml quartz cuvette containing 700-µl assay mixture[3]. A 120-mM potassium phosphate buffer pH 6.0 containing 1-mM EDTA under 100% N_2 was pre-incubated at 40°C for at least 5 min. Just before assay, 7.5 µl of 2-mM methylene-H_4MPT (the final concentration in the assay mixture was 20 µM) was added. The enzyme reaction was started by addition of 10-µl sample. Increase of the absorbance at 336 nm was measured. The specific activity was calculated using the extinction coefficient of methenyl-H_4MPT$^+$ ($\varepsilon_{336\,nm}$ = 21.6 $mM^{-1}cm^{-1}$) (ref [3]).

Mössbauer spectroscopy. The samples for Mössbauer spectroscopy were designed to simulate the initial buffer conditions of the crystallization drops. The sample in the absence of substrate contained 26-mg/ml [Fe]-hydrogenase (0.7 mM) about 60% enriched with ^{57}Fe, 10% w/v polyethylene glycol 3350, 50-mM tri-sodium citrate pH 4.0 and 100-mM tri-sodium citrate. The sample in the presence of methenyl-H_4MPT$^+$ contained 26-mg/ml [Fe]-hydrogenase about 60% enriched with ^{57}Fe, 10% w/v polyethylene glycol 3350, 100-mM sodium thiocyanate and 3-mM methenyl-H_4MPT$^+$. The concentrations shown above were the final concentration in the solution. In the anaerobic tent (95%N_2/5%H_2) the 0.7-ml sample solutions were transferred into a 0.7-ml Mössbauer cup each placed in a 250-ml brown bottle, which was subsequently sealed with a

rubber stopper and held with a screw cap. The gas phase in the bottles containing the sample with methenyl-H_4MPT^+ was exchanged via a needle by evacuation and refilling with 100% N_2 at 1.3 bar. The bottles were incubated at 4 °C for 1 h and then frozen at −75 °C for 1.5 h. The frozen samples in the Mössbauer cups were quickly transferred into a liquid nitrogen bath and subsequently stored in a Dewar filled with liquid nitrogen until measurements.

Data were collected on an alternating constant-acceleration spectrometer. The sample temperature was maintained constant in an Oxford Instruments Variox Mössbauer cryostat. All isomer shifts are quoted relative to iron metal at 300K. The zero-field spectra were fitted by using Lorentzian line shapes.

Infrared spectroscopy. The samples for infrared spectroscopy were prepared in amber-coloured 1.5-ml Eppendorf tubes. The sample solutions contained 150-mg/ml (4-mM) [Fe]-hydrogenase in 50-mM MES/NaOH pH 6.0 or 50-mM Tricine/NaOH pH 8.0, some of which contained 10-mM methenyl-H_4MPT^+ (final concentrations). The sample solutions were prepared in the anaerobic tent with the gas phase 95%N_2/5%H_2 and then the tubes were transferred into amber glass-bottles and the bottles were sealed with a rubber stopper and a screw cap. The gas phase of the bottles were exchanged with 100%N_2 by evacuation and refilling of the gas and then frozen in liquid nitrogen. The frozen samples in tubes were stored in a Dewar filled with liquid nitrogen until measurements.

All infrared spectra were obtained with an FTIR spectrometer (Bruker, Vertex 70V) in an attenuated total reflection (ATR) optical configuration with a Si prism of 45° incident angle and 2 active reflections (Smith Detection, DuraSamplIR IITM). Spectra were obtained with a resolution of 4 cm^{-1}. Five microliters of the sample solutions were dropped onto the effective area of a Si prism (3-mm diameter) and concentrated by slowly evaporating the solvent under mild flow of

argon gas. The hydration of the sample was estimated by the relative intensities of the water band (OH stretching mode) at approximately 3500 cm^{-1} against the amide II band of the protein at approximately 1550 cm^{-1}. Spectra were measured successively during the concentration process. We selected a spectrum of a mildly hydrated sample that provided enough intensity to analyse the cofactor bands. A baseline correction was made on the selected spectrum to eliminate contributions from the water overtone band approximately 2000 cm^{-1}. Typically, 512 spectra were averaged to obtain a sufficient signal-to-noise ratio. Measurements were performed in the dark by covering the spectrometer with blackout fabric to avoid light-induced decomposition of the sample. Intensities of the observed bands from various samples were at arbitrary concentrations. For quantitative comparison of the obtained spectra, intensities of the CO bands were normalized by the peak intensities of the amide II band of each spectrum.

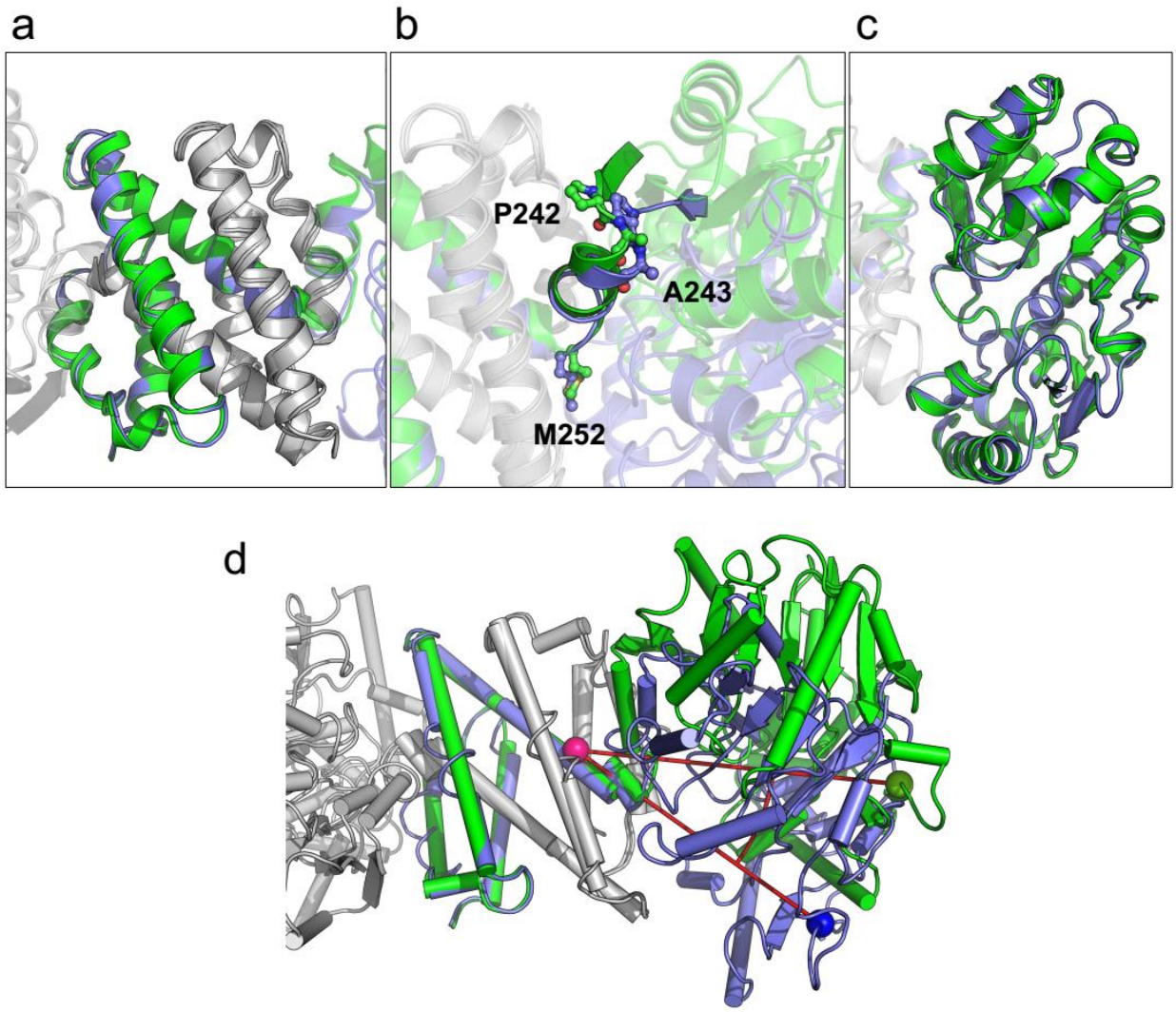

Supplementary Fig. 1 | Superposition of the domains of [Fe]-hydrogenase holoenzyme from *M. aeolicus* in the open and closed conformations. The structure of the open state (green cartoon) and that of the closed state in complex with the methenyl-H_4MPT^+ (blue cartoon) are compared. **a**, The central domain formed from two C-terminal segments, RMSD 0.34 Å for 77 Cα residues. **b**, The hinge region. **c**, The N-terminal domain binding the FeGP cofactor, RMSD 0.26 Å for 191 Cα residues. **d**, The relative arrangement of the N-terminal domains when using only the central domain for superposition. The rotation angle between them in the closed and open state is ~30°.

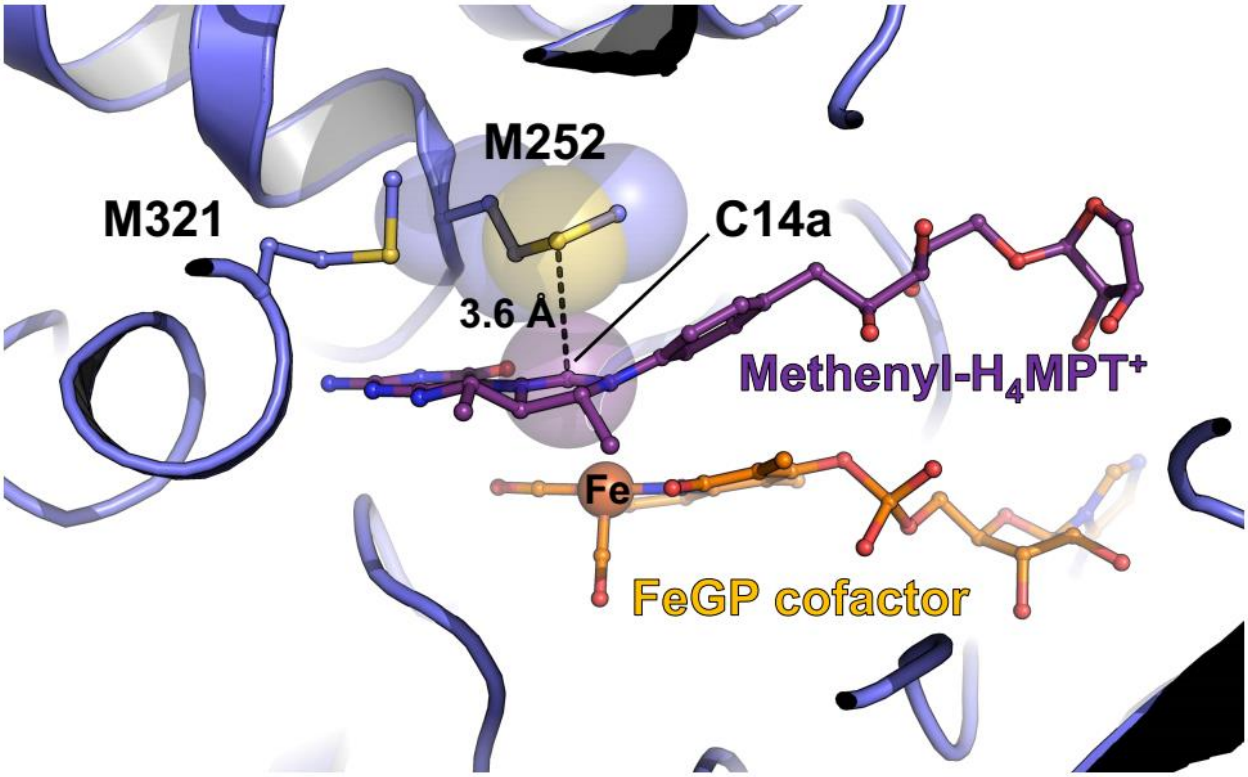

Supplementary Fig. 2 | Interactions of Met252 with the imidazoline ring of methenyl-H_4MPT^+ in the closed active structure of [Fe]-hydrogenase. In the closed conformation, the imidazoline part is stabilized by interactions with Met252 (van der Waals forces between S-CH_3 and C14a). The van der Waals radius of S-CH_3 of Met252 and C14a of methenyl-H_4MPT^+ is illustrated with transparent balls. Met252 (carbon in blue), Met321 (carbon in blue), methenyl-H_4MPT^+ (carbon in purple) and the FeGP cofactor (carbon in orange) are shown in sticks and balls, in which nitrogen, oxygen, sulphur and Fe atoms were depicted in dark blue, red, yellow and dark orange, respectively.

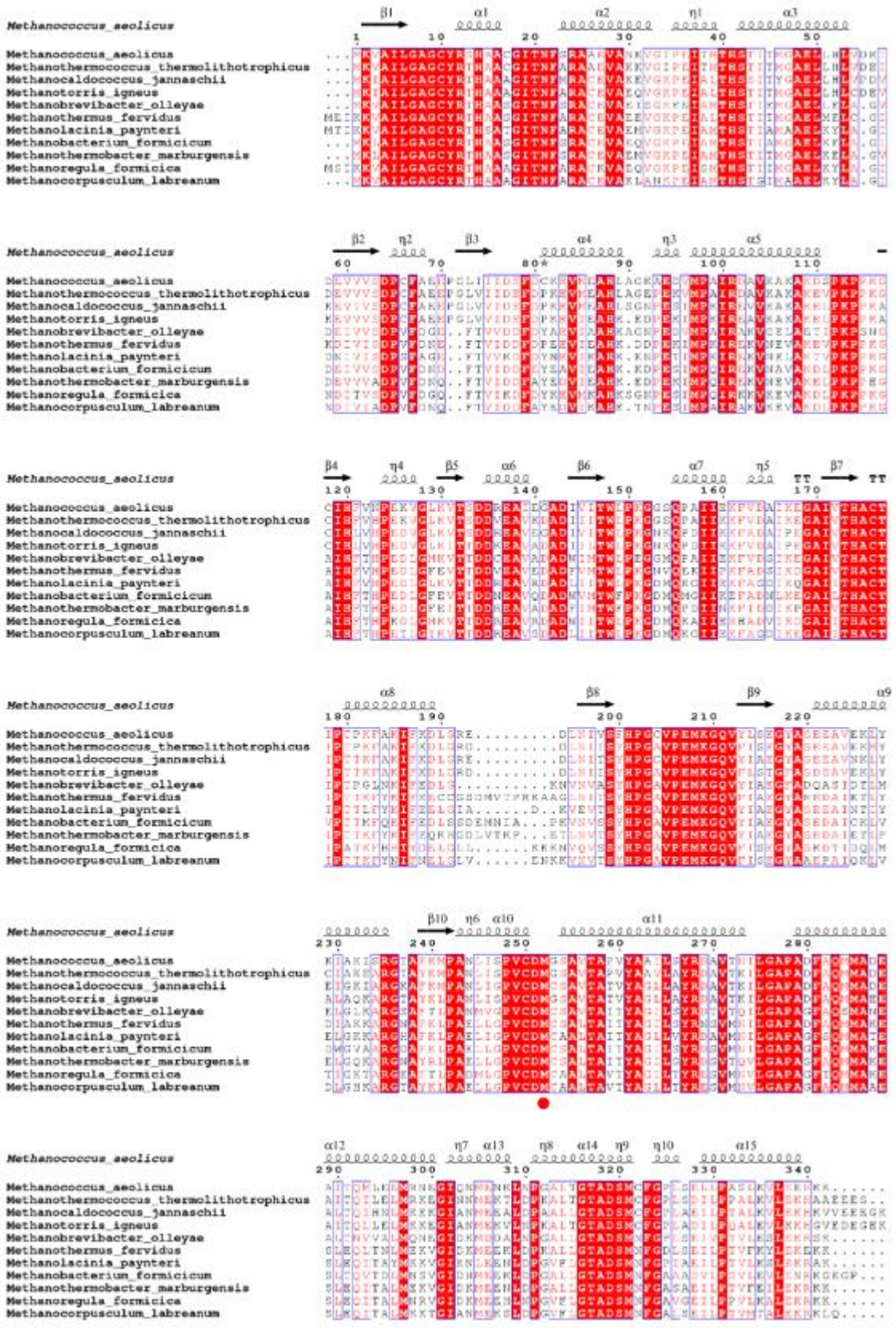
Methanococcus_aeolicus
Methanococcus_aeolicus
Methanothermococcus_thermolithotrophicus
Methanocaldococcus_jannaschii
Methanotorris_igneus
Methanobrevibacter_olleyae
Methanothermus_fervidus
Methanolacinia_paynteri
Methanobacterium_formicicum
Methanothermobacter_marburgensis
Methanoregula_formicica
Methanocorpusculum_labreanum

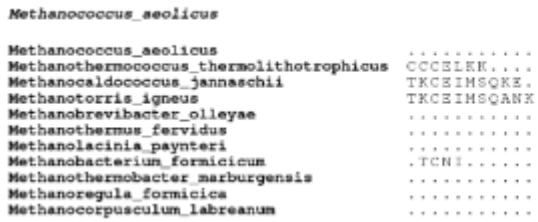

Supplementary Fig. 3 | Alignments of protein sequences of [Fe]-hydrogenases from different organisms. All sequences are from NCBI database. Alignments was performed by Clustal Omega (http://www.ebi.ac.uk/Tools/msa/clustalo/). The figure was generated by ESPript 3.0 (ref [4]). Met252 was strictly conserved in [Fe]-hydrogenase and marked with red closed circle in the figure.

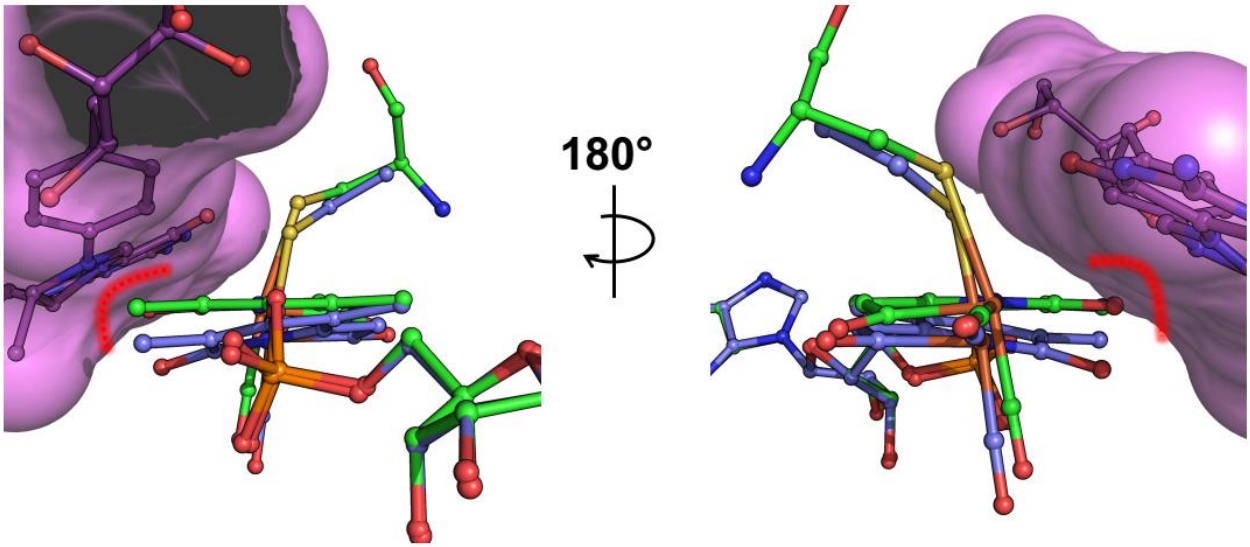

Supplementary Fig. 4 | Conformation of the FeGP cofactor and methenyl-H_4MPT^+ of the open and closed states of [Fe]-hydrogenase from *M. aeolicus*. Superposition of the FeGP cofactor in the open state (in green) and the closed state in complex with methenyl-H_4MPT^+ (in purple). The N-terminal domains were superimposed. The surface of the bulky methenyl-H_4MPT^+ is shown in light pink and the steric clashes with the FeGP cofactor in the open state is shown by a red dash curve.

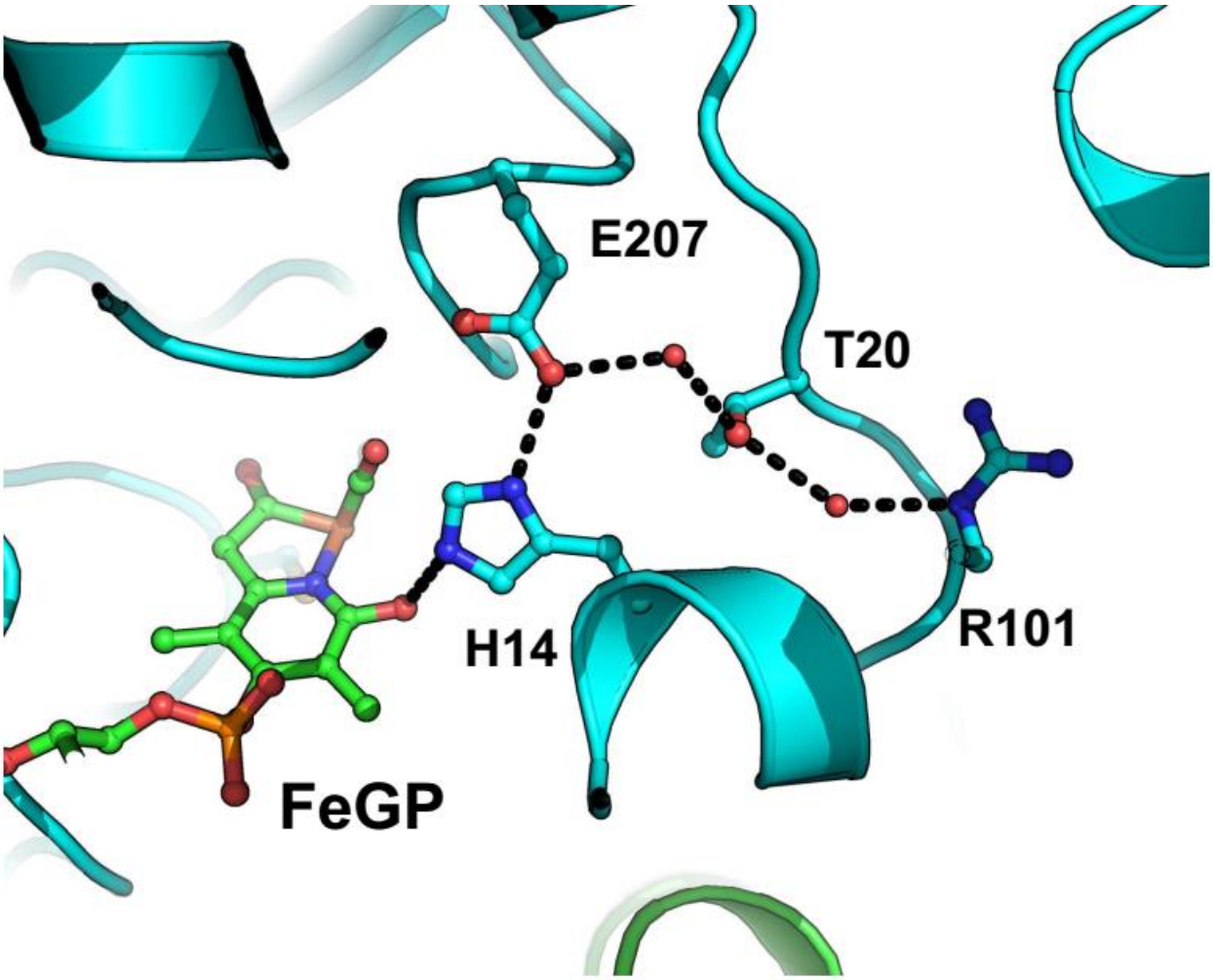

Supplementary Fig. 5 | Putative proton relay in the closed form of [Fe]-hydrogenase. This possible proton relay facilitates the transfer of the proton from 2-OH group of the pyridinol part of the FeGP cofactor (shown by black dashed-line). Methenyl-H_4MPT^+ is omitted for clarification.

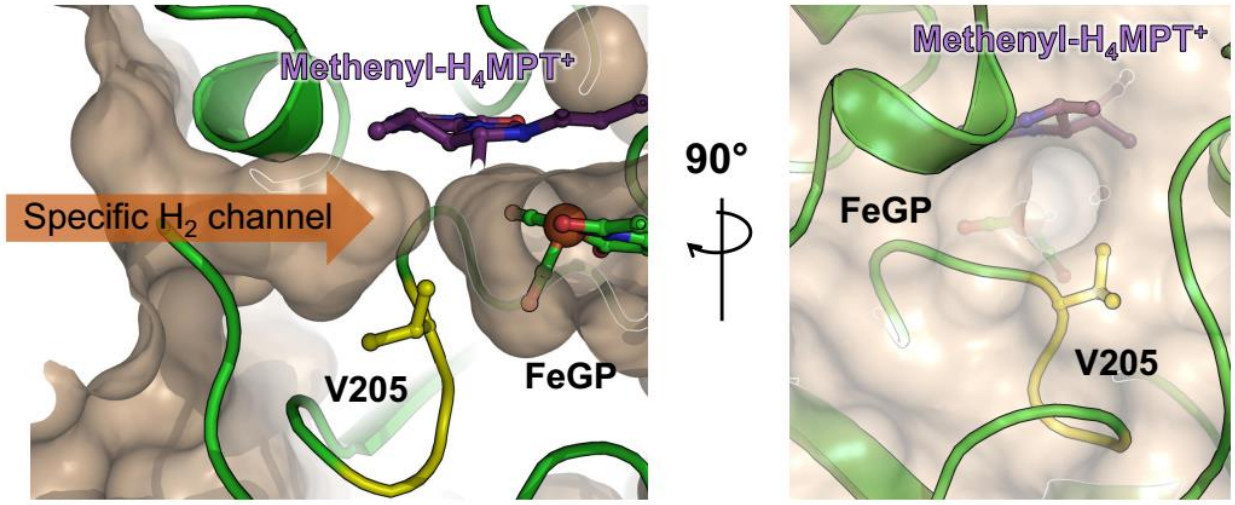

Supplementary Fig. 6 | Possible H_2 channel in the closed form. The surface of [Fe]-hydrogenase is shown in sand and the FeGP cofactor (Fe in a dark orange ball), methenyl-H_4MPT^+ (purple) and Val205 (yellow) are shown in balls and sticks. Val205 is strictly conserved in all [Fe]-hydrogenases (see Supplementary Fig. 3) and might serve as filter to block the entry of unwanted solutes or gases (for example, O_2).

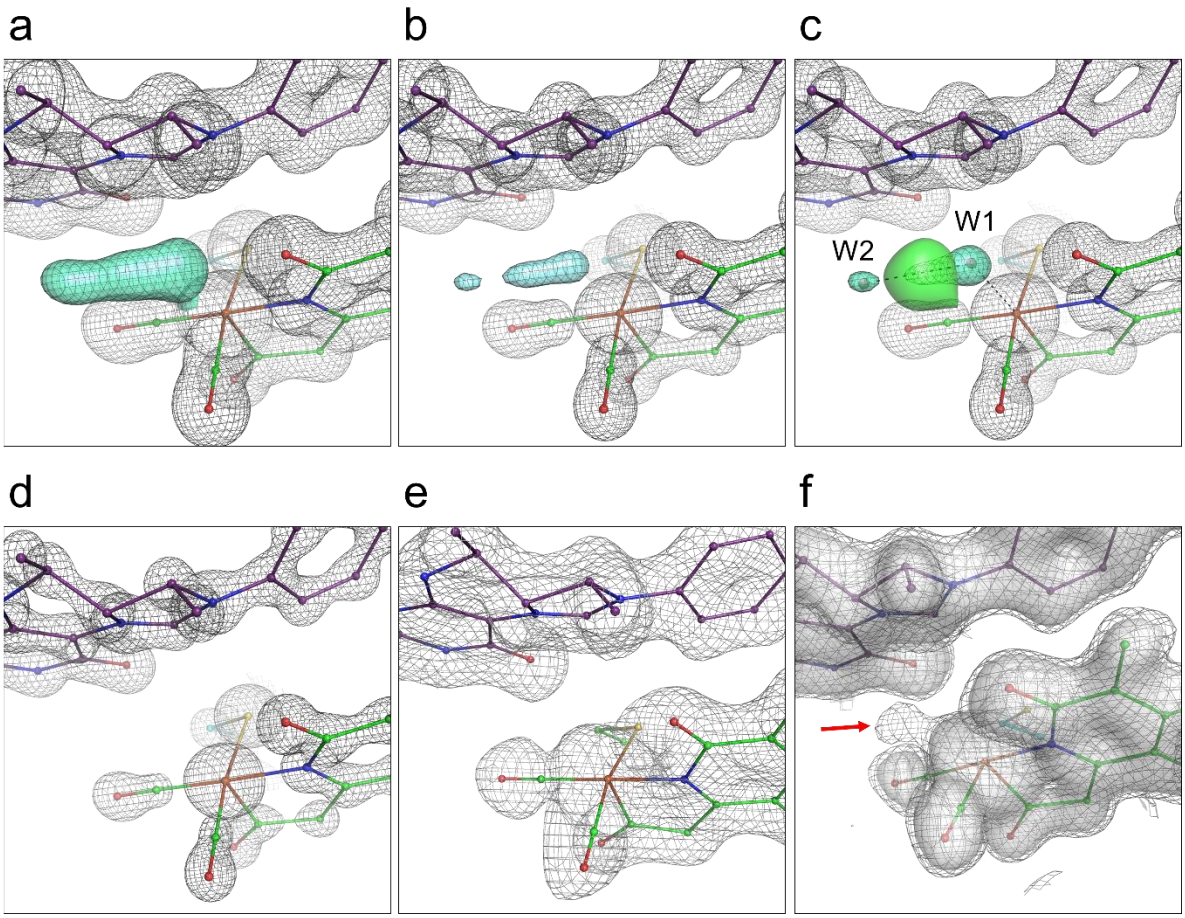

Supplementary Fig. 7 | $2F_o$-F_c electron density map of the FeGP cofactor (carbon atoms in green) and methenyl-H_4MPT$^+$ (carbon atoms in purple) in the closed form of [Fe]-hydrogenase. The contour level for form A (resolution 1.06 Å) is 1.0 σ in (**a**), 2.0 σ in (**b**), 3.0 σ in (**d**). In (**c**) two water molecules were modelled and refined with fixed B-factor of 15 Å² (which is the average B-factor for the carbon monoxide ligands of the FeGP) and an occupancy of 0.5 and 0.4 for water 1 (W1) and 2 (W2), respectively. The $2F_o$-F_c map (in grey mesh and cyan transparent surface) is contoured at 2.0 σ and the difference map between the two water molecules is contoured at 3.0 σ and highlighted by a green transparent surface. The extra difference density indicates that two water molecules cannot properly explain the $2F_o$-F_c density. In addition, the distance between W1-Fe is 2.1 Å and between W1-W2 is 2.4 Å. The contour level for form B (resolution 1.85 Å) is 1.0 σ for the first monomer of the dimer in the asymmetric unit (**e**) and 1.0 σ for the second monomer (**f**). A transparent surface corresponds to the map with a cut off at 1.5 σ. The extra electron density observed at 1.0 σ, which is bound to the Fe site (shown by a red arrow in **f**) disappears at 1.5 σ. This extra electron density might come from thiocyanate (200 mM in the crystallization solution). Thiocyanate did not inhibit [Fe]-hydrogenase from *M. aeolicus* at the used concentration.

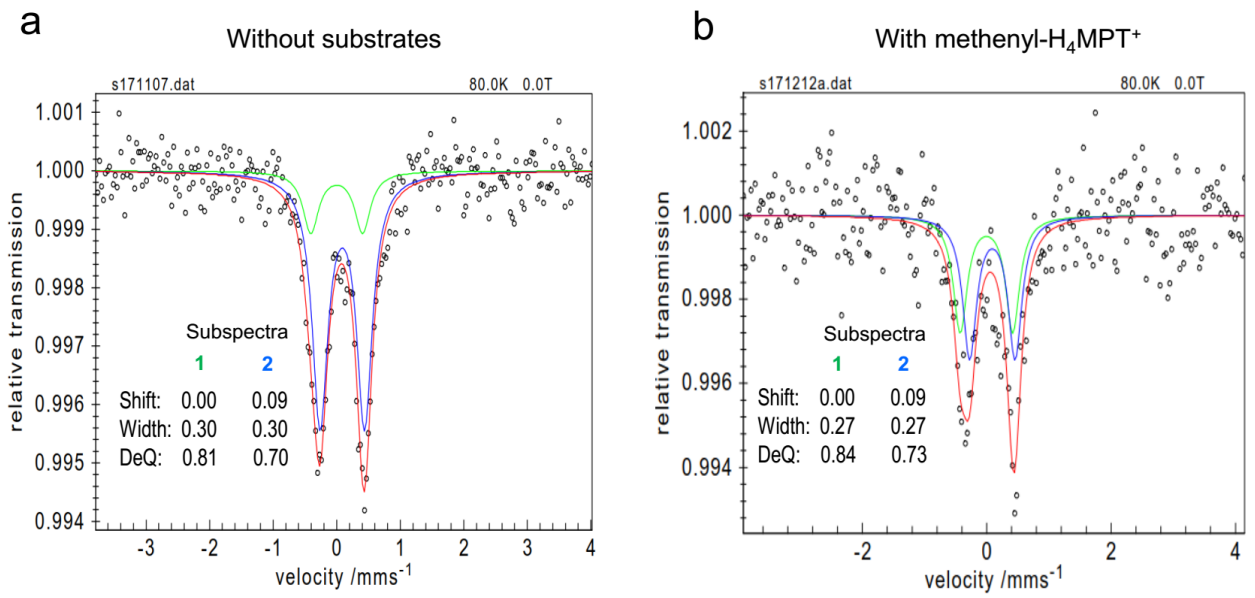

Supplementary Fig. 8 | Zero-field Mössbauer spectra of [Fe]-hydrogenase from *M. aeolicus* recorded at 80K. a, In the absence of substrates. **b**, In the presence of methenyl-H_4MPT^+. The Mössbauer parameters of each spectrum are shown in each panel: Shift: isomer shift; Width: Line width; DeQ: Quadrupole splitting are given in mm/s. Subspectrum 1 (green); subspectrum 2 (blue); superposition of subspectra (red); experimental spectrum (dots).

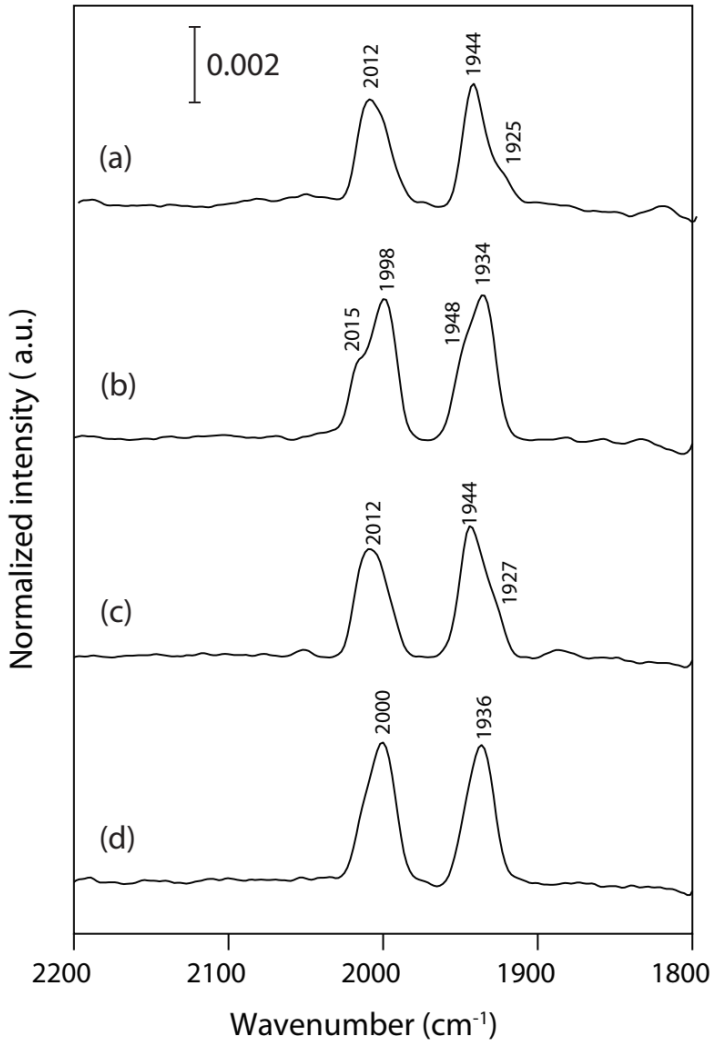

Supplementary Fig. 9 | Infrared spectra of [Fe]-hydrogenase from *M. aeolicus*. At pH 6.0 (50-mM MES/NaOH): **a**, in the presence of methenyl-H_4MPT^+ under 100% N_2; **b**, in the absence of methenyl-H_4MPT^+ under 100% N_2. At pH 8.0 (50-mM Tricine/NaOH): **c**, in the presence of methenyl-H_4MPT^+ under 100% N_2; **d**, in the absence of methenyl-H_4MPT^+ under 100% N_2.

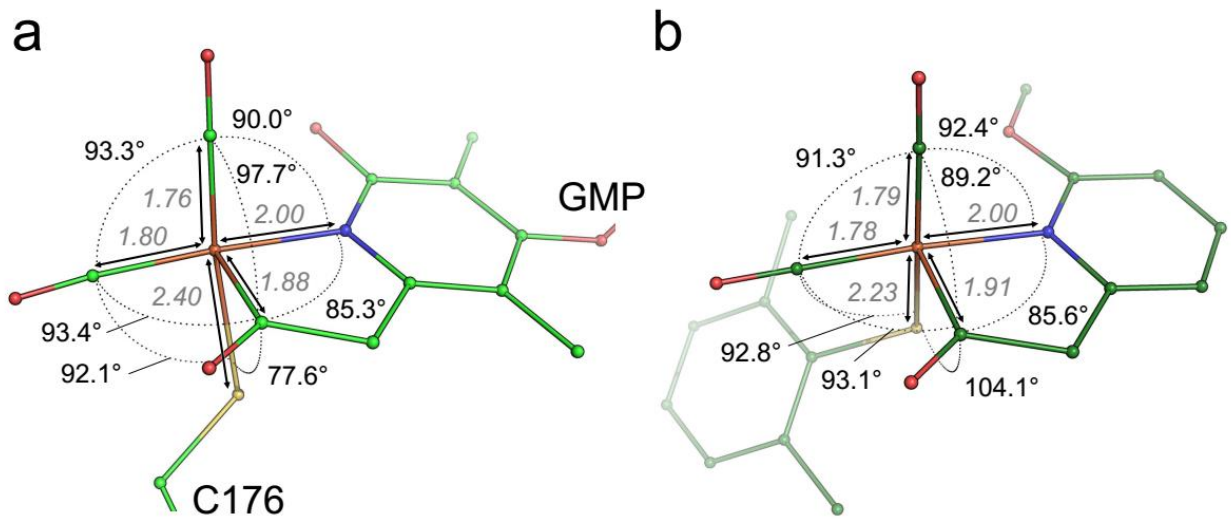

Supplementary Fig. 10 | Coordination of the penta-coordinated iron complex structures. **a**, The FeGP cofactor in [Fe]-hydrogenase in the closed form. **b**, A mimic complex (2-CH_2CO-6-$MeOC_5H_3N$)$Fe(CO)_2$[S-(2,6-$Me_2C_6H_3$)] (ref [5]). The structures were shown in sticks and balls, in which carbon, nitrogen, oxygen, sulphur and Fe atoms were depicted in green, dark blue, red, yellow and orange, respectively.

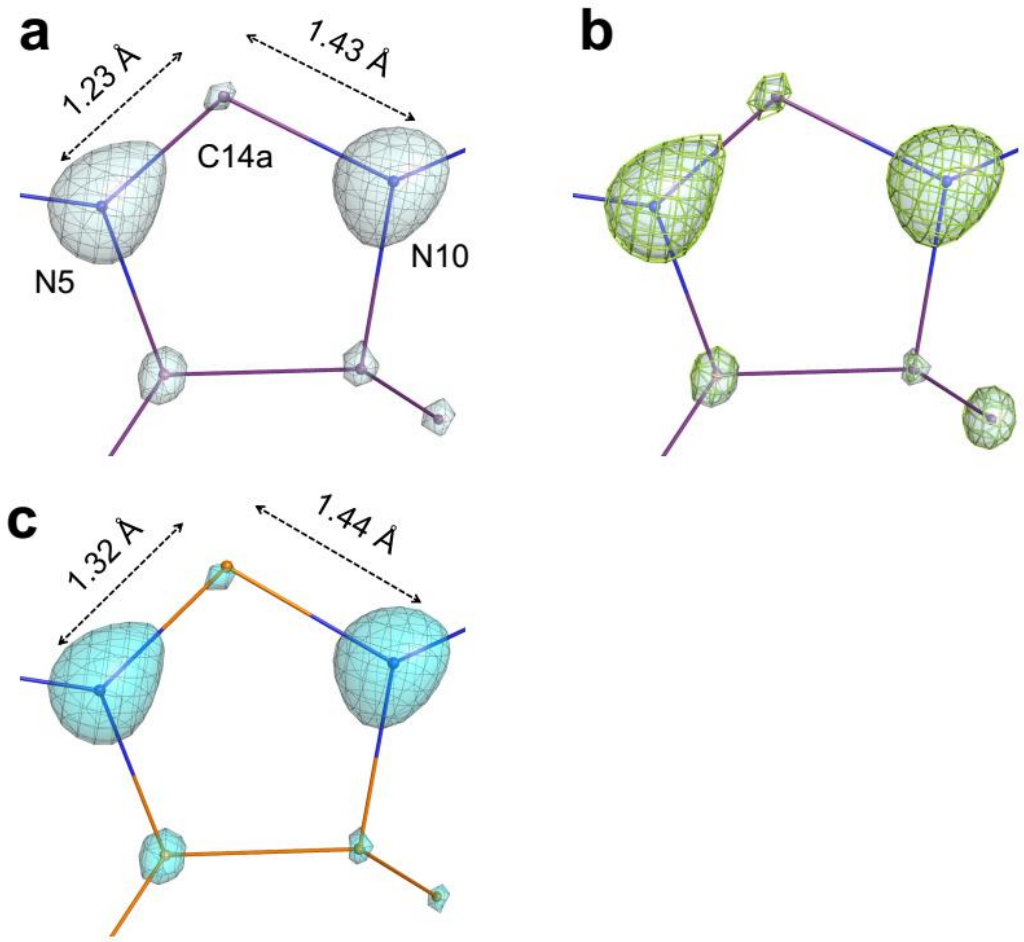

Supplementary Fig. 11 | Representation of the electron density around the C14a of the methenyl-H_4MPT$^+$ in the closed form. a, Methenyl-H_4MPT$^+$ in ball and stick representation and a 2F_o-F_c map contoured at 5.3 σ after refinement with best modelled substrate conformation. **b**, Same representation of **a**, with a 2*Fo-Fc* omit map contoured at 4.4 σ (in surface and grey mesh) and the F_o-F_c omit map contoured at 15.2 σ highlighted as a green mesh. **c,** Same representation as in **a** but using an idealized methenyl-H_4MPT$^+$ containing the classic double bond C14a=N5 distance of 1.32 Å. The 2F_o-F_c map after refinement with this restrained model is contoured at 5.3 σ. It is worthwhile to note the C14a position outside the electron density attests a shorter N5-C14A double bond.

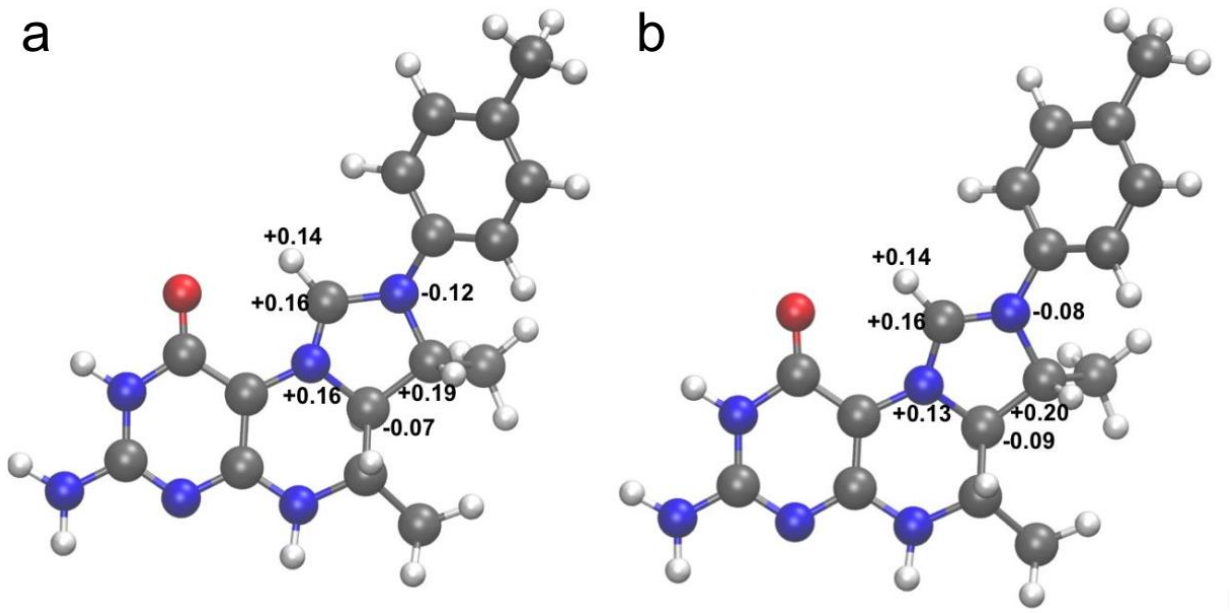

Supplementary Fig. 12 | Iterative Hirshfeld atomic charges for the methenyl-H_4MPT$^+$ of closed [Fe]-hydrogenase. In the fixed conformation (**a**) and fully relaxed geometries (**b**). Charges obtained through DFT computations at the PBE0/def2-SVP level. The structures were shown in sticks and balls, in which carbon, nitrogen, oxygen, and hydrogen atoms were depicted in grey, blue, red and white, respectively.

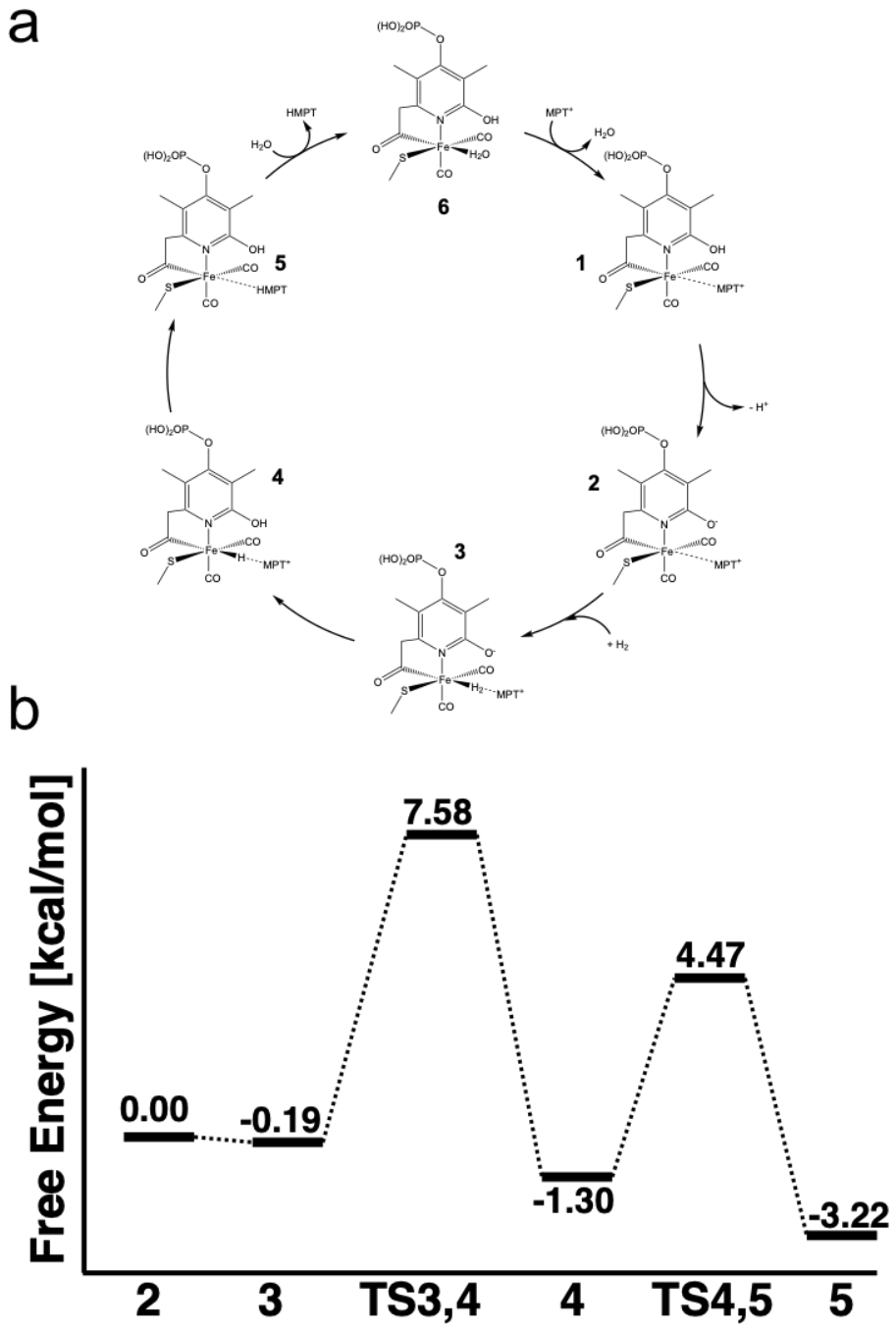

Supplementary Fig. 13 | Computed free energy profile for a portion of the catalytic cycle. **a**, The proposed catalytic cycle of [Fe]-hydrogenase on the basis of truncated forms of the FeGP cofactor and methenyl-H_4MPT^+ (MPT^+). **b**, QM/MM computed free energy profile for a portion of the catalytic cycle. See computational details in Methods for a full overview of the employed computational protocol. The atomic coordinates of the optimized computational models (Step 2-5, TS3,4 and TS4,5) are available from the Supplementary Data Files 1-6.

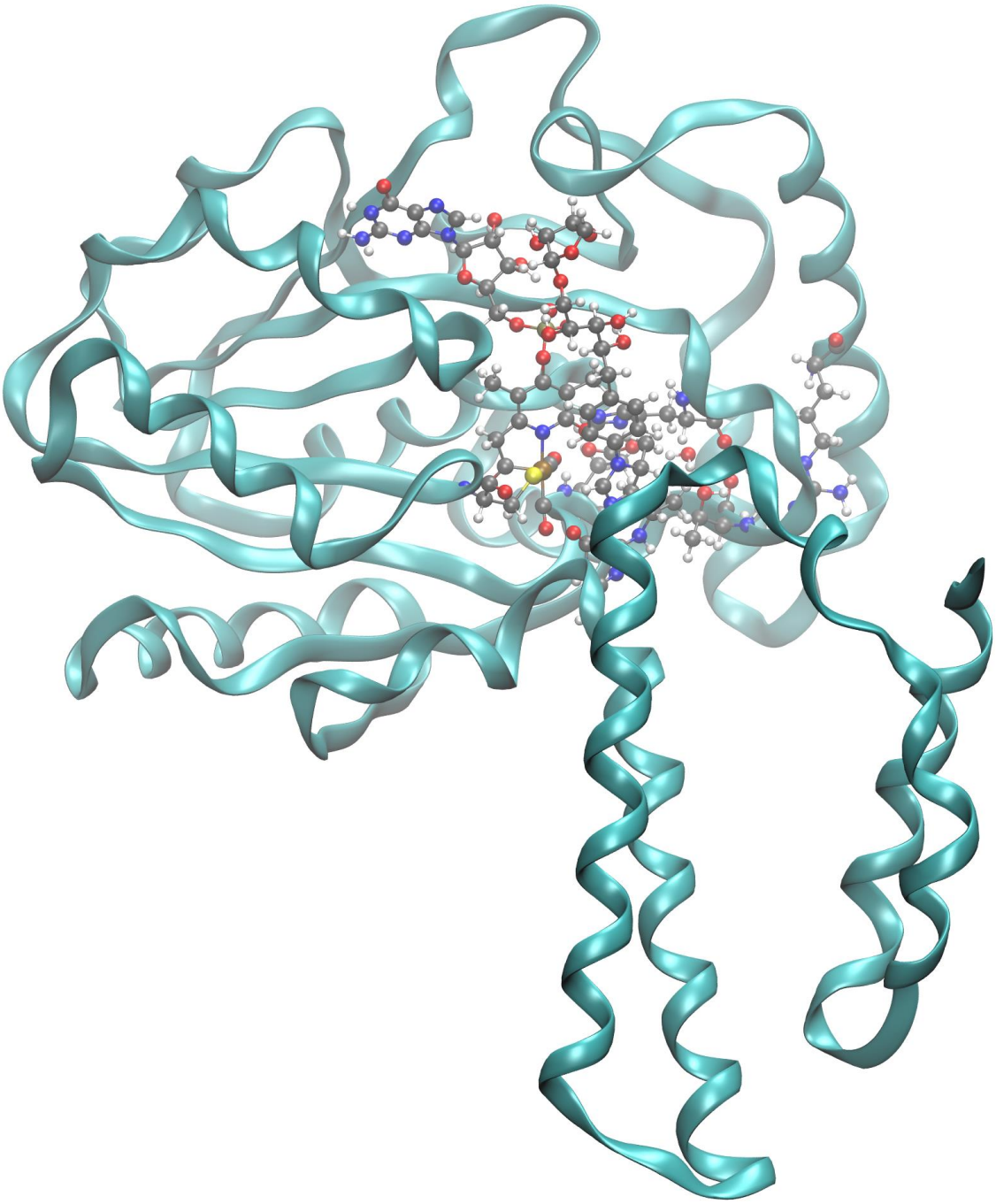

Supplementary Fig. 14 | QM/MM optimized geometry of the active site in step 2. Cofactors, substrates, and amino acid residues relevant to the catalytic process are shown as ball and sticks, while the remainder of the protein is drawn in ribbon form. Cofactor- and substrate-structures of relevant catalytic cycle using fixed closed geometry. Carbon, nitrogen, oxygen, sulphur, phosphate, hydrogen and iron atoms are depicted in grey, blue, red, yellow, gold, white and brown, respectively. The atomic coordinates of the optimized computational model (step 2) is available from the Supplementary Data Files 1-6.

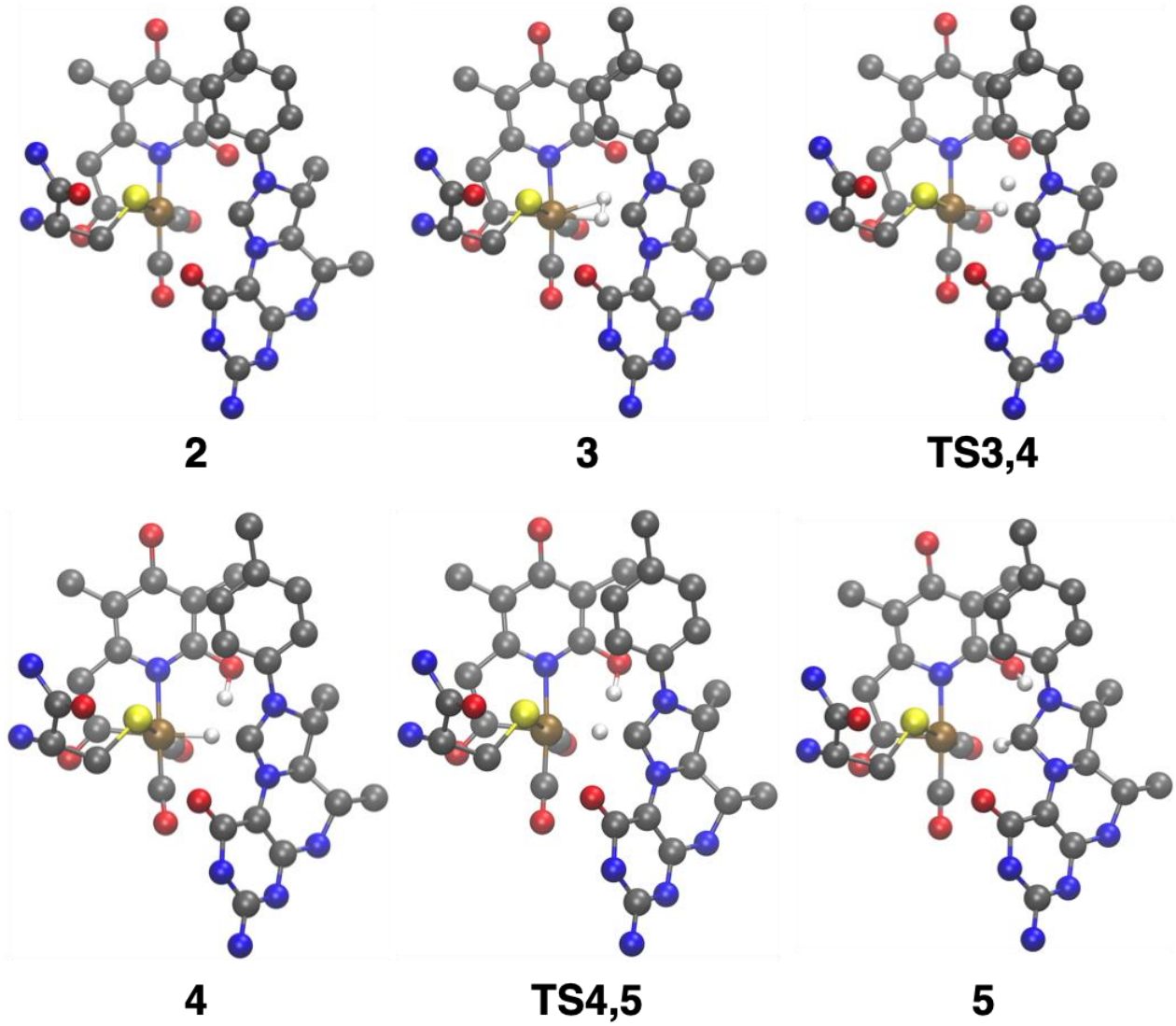

Supplementary Fig. 15 | QM/MM optimized geometries of the cofactor- and substrate-structure of relevant catalytic cycle intermediates and transition states. Note that, for clarity, only the heavy atoms and relevant hydrogen atoms are shown. The protein structure is present, as depicted in Supplementary Fig. 14. Carbon, nitrogen, oxygen, sulphur, hydrogen and iron atoms are depicted in grey, blue, red, yellow, white and brown, respectively. The atomic coordinates of the optimized computational models (Step 2-5, TS3,4 and TS4,5) are available from the Supplementary Data Files 1-6.

Supplementary Table 1 | X-ray analysis statistics.

	[Fe]-hydrogenase Open conformation	[Fe]-hydrogenase with methenyl-H_4MPT^+ Closed conformation Form A	[Fe]-hydrogenase with methenyl-H_4MPT^+ Closed conformation Form B
Data collection			
Wavelength (Å)	0.97980	1.00001	0.99992
Space group	$I4_122$	$C222_1$	$P2_12_12$
Resolution (Å)	50 – 2.30 (2.42 – 2.30)	47 – 1.06 (1.12 – 1.06)	45 – 1.85 (1.95 – 1.85)
Cell dimensions			
a, b, c (Å)	136.99, 136.99, 117.32	66.65, 66.25, 167.60	80.01, 156.48, 53.65
α, β, γ (°)	90.0, 90.0, 90.0	90.0, 90.0, 90.0	90.0, 90.0, 90.0
R_{merge} (%)[a]	15.5 (102.3)	4.9 (98.1)	12.4 (113.3)
R_{pim} (%)[a]	4.3 (28.1)	2.1 (54.2)	5.5 (62.7)
$CC_{1/2}$ (%)[a]	99.9 (60.2)	99.9 (67.2)	99.7 (32.3)
I/σ_I[a]	17.9 (2.9)	15.4 (1.4)	8.6 (1.2)
Completeness (%)[a]	100.0 (100.0)	93.7 (74.8)	97.4 (85.0)
Redundancy[a]	13.7 (14.0)	6.1 (4.0)	6.0 (4.1)
Number of unique reflections[a]	25078 (3607)	156432 (18054)	56771 (6994)
Refinement			
Resolution (Å)	26.62 – 2.30	45.0 – 1.06	45.0 – 1.85
Number of reflections	25043	156000	56710
R_{work}/R_{free}[b] (%)	17.1 / 19.2	11.8 / 13.4	16.1 / 19.2
Number of atoms			
Protein	2573	2776	5173
Ligands/ions	66	136	264
Solvent	107	505	592
Mean B-value ($Å^2$)	43.63	19.10	28.83
Molprobity clash score, all atoms	2.45 (100^{th} percentile)	4.38 (79^{th} percentile)	1.48 (100^{th} percentile)
Ramachandran plot			
Favoured regions (%)	326 (95.9)	326 (96.5)	656 (96.5)
Outlier regions (%)	0	0	0
rmsd[c] bond lengths (Å)	0.009	0.011	0.010
rmsd[c] bond angles (°)	1.11	1.42	1.11
PDB code	6HAC	6HAV	6HAE

[a] Values relative to the highest resolution shell are within parentheses. [b] R_{free} was calculated as the R_{work} for 5% of the reflections that were not included in the refinement. [c] rmsd, root mean square deviation.

Supplementary Table 2 | The catalytic activity of the [Fe]-hydrogenase variants from *M. aeolicus.*

Enzyme	Specific activity (U/mg)	Residual activity (%)
Wild type	3000	100
Met252Ala	14	0.5
Met252Ser	37	1.2
Met252Phe	4	0.1

The specific activity of the oxidation of methylene-H_4MPT to methenyl-H_4MPT^+ was measured at 40 °C. One unit of the activity corresponds to the formation of one μmol of methenyl-H_4MPT^+ per min.

Supplementary Table 3 | Computed free energies of relevant species. Values in hartree. The atomic coordinates of the optimized computational models (Step 2-5, TS3,4 and TS4,5) are available from the Supplementary Data Files 1-6.

Species	M06/6-31G(d,p)//UFF QM/MM Free Energies (298K)
H_2	-1.166944
2	-4185.815488
3	-4186.998128
TS3,4	-4186.998438
4	-4187.006827
TS4,5	-4186.990501
5	-4187.004461

Supplementary References

1 Shima, S. & Thauer, R. K. Tetrahydromethanopterin-specific enzymes from *Methanopyrus kandleri*. *Methods Enzymol.* **331**, 317-353 (2001).

2 Moore, J. T., Uppal, A., Maley, F. & Maley, G. F. Overcoming inclusion body formation in a high-level expression system. *Protein Expres. Purif.* **4**, 160-163 (1993).

3 Shima, S., Schick, M. & Tamura, H. Preparation of [Fe]-hydrogenase from methanogenic archaea *Methods Enzymol* **494**, 119-137 (2011).

4 Robert, X. & Gouet, P. Deciphering key features in protein structures with the new ENDscript server. *Nucleic Acids Res.* **42**, W320-W324 (2014).

5 Chen, D. F., Scopelliti, R. & Hu, X. L. A five-coordinate iron center in the active site of [Fe]-hydrogenase: hints from a model study. *Angew. Chem. Int. Ed.* **50**, 5671-5673 (2011).